Catal Lett (2007) 119:95–100
DOI 10.1007/s10562-007-9202-x

Dehydrogenation of Cyclohexene on Platinum Nanoclusters on a Thin Film of Al_2O_3/NiAl(100)

Shrikrishina D. Sartale · Huang-Wei Shiu · Wen-Hua Wen · Meng-Fan Luo · Y. C. Lin · Yao-Jane Hsu

Received: 7 March 2007 / Accepted: 29 June 2007 / Published online: 25 July 2007

Abstract Using a scanning-tunneling microscope, reflection high-energy electron diffraction and photoelectron spectra with synchrotron radiation, we investigated the temperature dependence of the dehydrogenation of cyclohexene (C_6H_{10}) adsorbed on Pt nanoclusters supported on an ultra-thin film of Al_2O_3/NiAl(100). The Pt clusters, grown by vapor deposition, are structurally ordered and exhibit a mean diameter 2.2 nm and height 0.4 nm. The progress of dehydrogenation was monitored through the temporal variation of C 1s photoelectron spectra; analysis of these features revealed that the dehydrogenation of cyclohexene with increasing sample temperature occurs as a sequential process beginning around 150 K, a temperature significantly less than that for Pt single-crystal surfaces. The dehydrogenation behavior, particularly the decomposition into elemental carbon, is found to vary with Pt coverage.

Keywords Dehydrogenation · Cyclohexene · Pt · Nanocluster · STM · PES

S. D. Sartale · H.-W. Shiu · W.-H. Wen · M.-F. Luo (✉)
Department of Physics and Center for Nano Science and Technology, National Central University, 300 Jhongda Road, Jhongli 32001, Taiwan, China
e-mail: mfl28@phy.ncu.edu.tw

Y. C. Lin · Y.-J. Hsu
National Synchrotron Radiation Research Center, 101 Hsin-Ann Road, Hsinchu Science Park, Hsinchu 30076, Taiwan, China

Y. C. Lin
e-mail: yjhsu@nsrrc.org.tw

1 Introduction

Because of the relevance to petroleum processing [1–11], the dehydrogenation of cyclic hydrocarbons such as cyclohexane (C_6H_{12}) and cyclohexene (C_6H_{10}) over single-crystal Pt(100) and Pt(111) surfaces has been extensively investigated with various techniques. Cyclohexene, a possible intermediate in the dehydrogenation of cyclohexane into benzene, can be hydrogenated to cyclohexane or dehydrogenated to benzene (C_6H_6). Under ultrahigh vacuum (UHV) conditions, cyclohexene adsorbs on Pt(111) or Pt(100) surfaces at 100 K and exists in di-σ cyclohexene form. At about 200 K, di-σ cyclohexene converts to π-allyl c-C_6H_9 and at about 300 K dehydrogenates to benzene [9]. On further heating, some benzene desorbs from the surface at 400–500 K, and the remaining benzene decomposes to hydrogen and adsorbed carbon.

Such experiments with single Pt crystals have contributed much to the understanding of dehydrogenation, but their practical value is limited. Many aspects are neglected in modeling the surface of a catalyst as that of a single crystal [12–14]; the most obvious is the absence of a support material. Furthermore, the properties of the surface of a small metallic particle might be poorly represented as their single-crystal counterparts; on a small particle various facets are present, and the density of edge and corner sites is much greater than on a single-crystal surface of small index. Finally, the electronic structure of small particles differs from that of large crystals [15]: the evolution from metallic to insulating behavior with the size of a particle can significantly influence the catalytic properties [16, 17]. A more realistic model for a supported catalyst thus consists of metallic particles of nanometer scale on well ordered oxide surfaces, as they contain both components and the heterogeneous character of most industrial cata-

lysts. Here we report our investigation of the dehydrogenation of cyclohexene on Pt nanoclusters supported on a thin film of Al_2O_3/NiAl(100). Al_2O_3 as an ultra-thin film grown on NiAl alloy, instead of bulk Al_2O_3, serves as support because we thereby avoid a charging effect arising during characterization with electronic spectrometric methods. Moreover, its electronic properties are not critically influenced by the alloy substrate [18].

The Pt clusters were formed by vapor deposition; their morphologies and crystallinity were characterized with a scanning-tunneling microscope (STM) and reflection high-energy electron diffraction (RHEED), respectively [19, 20]. The Pt clusters show a mean diameter 2.2 nm and height 0.4 nm [19], and have the fcc phase; the clusters grow with their (001) plane parallel to the θ-Al_2O_3 (100) surface, and with the [110] axis parallel to [010] directions of the oxide surface (Pt(001)[110]//Al_2O_3(100)[010]) [20]. We investigated the temperature dependence of the cyclohexene dehydrogenation by increasing the sample temperature in a stepwise manner and recording a photoelectron spectrum from the reaction mixture on the surface at each temperature step. Analysis of C 1s photoelectron spectra (PES), generated with synchrotron radiation, provided information about the surface species as the reaction progressed. The results indicate that the dehydrogenation of cyclohexene over the Pt clusters is a sequential process beginning around 150 K and ending with elemental carbon at 300–400 K. Both characteristic temperatures are significantly less than those for Pt single crystals, implying smaller activation energies and thus greater catalytic reactivity for the supported Pt clusters. We mention also the effects of the Pt coverage and of the temperature of cluster growth on the dehydrogenation.

2 Experiments

The NiAl(100) sample (MaTech GmbH) was polished to a roughness less than 0.03 μm and orientation accuracy better than 0.1°. All experiments were conducted in UHV chambers with base vacuum better than 1×10^{-9} torr. The deposition of Pt and the growth of a θ-Al_2O_3 thin film on NiAl(100) were performed as described previously [19–22]; the only difference is that the Al_2O_3 thin film on NiAl(100) was not subjected to protracted annealing post oxidation, thus preventing NiAl facets becoming exposed on the surface [21, 22].

Images with a STM (RHK UHV 300), as constant-current topography, were recorded at 90 K using a typical sample bias voltage +2.5 V and tunneling current 0.2 nA. The STM tip consisted of electrochemically etched tungsten wire. The rate of deposition of Pt was fixed at 0.12 ± 0.003 ML/min, calculated from the Pt coverage near 295 K. The Pt cluster coverages were estimated from the volume of the Pt clusters on crystalline Al_2O_3 observed with the STM (1 ML corresponds to a real density of fcc Pt(100) surface atoms, 1.3×10^{15} atoms/cm^2). The RHEED measurements were performed with an incident electron beam of energy 40 keV at a grazing angle 2–3° to the surface.

After deposition of Pt, the sample was transferred for PES measurements to the analysis chamber equipped with a nine-channel hemispherical electron analyzer (VG Scientific). Combining electron-bombardment heating and liquid-nitrogen cooling, the sample temperature was variable between 120 and 1500 K. When the substrate was cooled to approximately 120 K, it was exposed to cyclohexene (1–10 L; 1 Langmuir (L) = 1×10^{-6} torr s) on filling the analysis chamber to a background pressure $\approx 1 \times 10^{-8}$ torr. Cyclohexene (99.9%, Merck) was purified with several cycles of freezing, pumping and thawing. After exposure to cyclohexene at 120 K, the sample was annealed to various temperatures for 1 min and re-cooled to 120 K for PES measurements.

All PES spectra were recorded with the analysis chamber connected to the wide-range spherical-grating monochromator beamline (WR-SGM) and U5-spectroscopy beamline at National Synchrotron Radiation Research Center (NSRRC). The beamlines deliver soft X-ray photons with energy in a range 10–1500 eV (WR-SGM) and 60–1400 eV (U5) respectively. The total energy resolution, including the beamline and energy analyzer, was estimated to be better than 0.3 eV [23]. A fixed photon energy 380 eV was used throughout the experiments. The incident beam was along the surface normal and the photoelectrons were collected at an angle 50° from the surface normal. All PES data presented here were first normalized to the photon flux. The references for binding energies (BE) in all spectra were a substrate Ni $3p_{3/2}$ signal at 67 eV and an Al 2p signal at 72.9 eV. After linear background subtraction using Gaussian-Lorentzian functions, the spectra features were fitted with a nonlinear least-squares algorithm.

3 Results and Discussion

Morphologies and size distributions of the Pt clusters manifested by STM are similar to those observed earlier [19]. Randomly distributed Pt nanoclusters, with a mean diameter of 2.25 nm and height of 0.4 nm (standard deviation 0.5 nm for the diameter distribution and 0.15 nm for the height distribution), are seen to grow on a crystalline Al_2O_3 surface at any temperature in a range 300–600 K and at any coverage less than the coalescence level. The proportion of large clusters is enhanced at a large coverage, up to 2 ML, or growth temperature, up to 600 K, whereas

the size of most clusters remained about the mean [19]. The inset of Fig. 1 presents a typical STM image for the Pt clusters. Our RHEED measurements indicate that these Pt clusters are structurally ordered, in a fcc phase, and have their (001) planes parallel to the θ-Al_2O_3 (100) surfaces and [110] axes parallel to the [010] directions of the oxide surface, so Pt(001)[110]// Al_2O_3(100)[010] [20]. Figure 2 displays an example of the RHEED patterns obtained from Pt (about 0.5 ML) on Al_2O_3/NiAl(100). The RHEED patterns are derived at both (a) [0–10] and (b) [0–11] azimuths and the diffraction spots from the Pt clusters appear as indicated in the figure; detailed analysis is available in [20]. In contrast, PES spectra show no evident Pt 4f feature, generally employed to monitor the Pt deposited on the surface, because their binding energies (BE = 74.52 and 71.2 eV for bulk Pt $4f_{5/2}$ and Pt $4f_{7/2}$ respectively) [24] overlap closely those of Al^{ox} 2p and Al 2p (75.4 and 72.9 eV) from an Al_2O_3 thin film and the NiAl alloy substrate. We noticed, however, that the intensities of spectral features centered about 75.4 and 72.9 eV are significantly enhanced after a large deposition of Pt, as demonstrated in Fig. 1. The inset is the corresponding STM image from the surface. As the cross section for photoionization of Pt 4f (5.5 megabarn (Mb)/atom) is much greater than that for Al 2p (0.8 Mb/atom) at the photon energy used for the current measurements (380 eV) [25], we speculate that the Pt 4f core-level signals are superimposed on Al^{ox} 2p and Al 2p signals. As the Ni 3p signals remained almost the same, such an intensity enhancement must not be due to a greater intensity of the radiant beam or other experimental artifact.

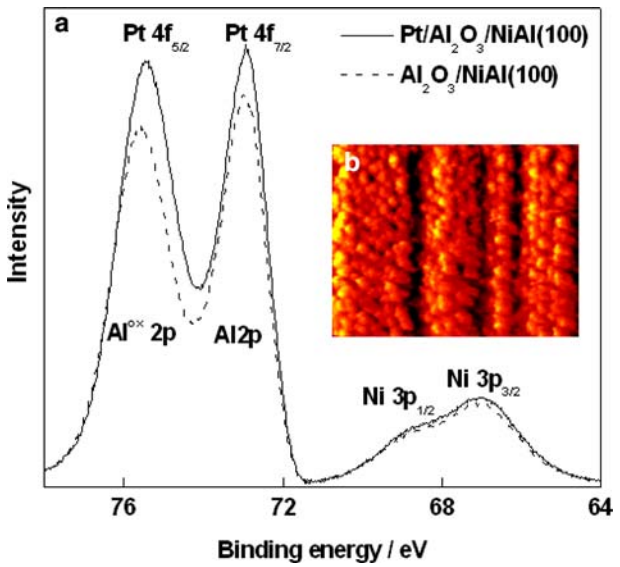

Fig. 1 (**a**) Representative photoelectron spectra for a pure thin film of Al_2O_3/NiAl(100) and Pt nanoclusters (2 ML) formed at 300 K on an Al_2O_3/NiAl(100) thin film. (**b**) Inset, representative STM image from Pt (2 ML), recorded at 90 K (image size 50 × 80 nm, bias = 2.5 V, I = 0.2 nA)

We tested the temperature dependence of dehydrogenation by increasing the sample temperature in a stepwise manner and recording a photoelectron spectrum from the reaction mixture on the surface at each temperature step. After adsorption of various amounts of cyclohexene at 120 K, we annealed the sample to a selected temperature, up to 500 K. The dehydrogenation induced upon annealing was reflected by a variation of the C 1s core level in the derived photoelectron spectra. Figure 3 displays C 1s photoelectron spectra in a typical series for cyclohexene (1 L) adsorbed over Pt clusters (~2 ML, formed at 300 K) supported on an Al_2O_3/NiAl(100) thin film and subsequently annealed to varied temperatures, as indicated in the figure. After exposure to cyclohexene, a symmetric C 1s signal appeared at a BE about 286 eV, comparable with the value observed over Pt black samples [26]. Slight annealing to 150 K leads to a substantially decreased intensity (see the noise level) of the C 1s signal, mainly due to desorption of multi-layers of cyclohexene from the surface. We confirmed this desorption by experiments with varied dosages of cyclohexene. Further annealing caused a continuously decreased intensity. With the annealing temperature the maximum of the C 1s signal also shifted toward lower BE, accompanied by an increased asymmetry and full width at half maximum (FWHM) of the line. These changes are explicitly plotted in Fig. 4. Such a continuous red shift (Fig. 4(a) of the BE indicates dehydrogenation of the cyclohexene. This assignment is further strengthened by the evident broadening of the signal in Fig. 4(b), implying the co-existence of various hydrocarbon species. The continuous change implies a continuous process, in contrast with earlier observations on Pt single crystals [1–5] but consistent with a mechanism of dehydrogenation proposed on the basis of thermochemical calculations for cyclohexene on a Pt(111) surface [6]. There, adsorbed cyclohexene loses H atoms stepwise to form a cycloallylic species (c-C_6H_9), cyclohexadiene (c-C_6H_8), cyclohexadienyl (c-C_6H_7) and then benzene (C_6H_6). The dehydrogenation notably begins at 150 K, much lower than the temperature for a single-crystal surface [1–11]. The dissociation of benzene, evident through the shift of the C 1s signal to the elemental carbon position about 284.5–285 eV, occurs between 300 and 400 K, also a lower temperature than expected for Pt single crystals [9]. The lower characteristic temperatures indicate smaller activation energies for both dehydrogenation of cyclohexene and decomposition of benzene. Because the above spectral features were not observed for a bare Al_2O_3 surface, the dehydrogenation must occur on the Pt clusters or at the Pt-oxide interface. We thus conclude that oxide-supported Pt nanoclusters are catalytically more active than Pt single crystals.

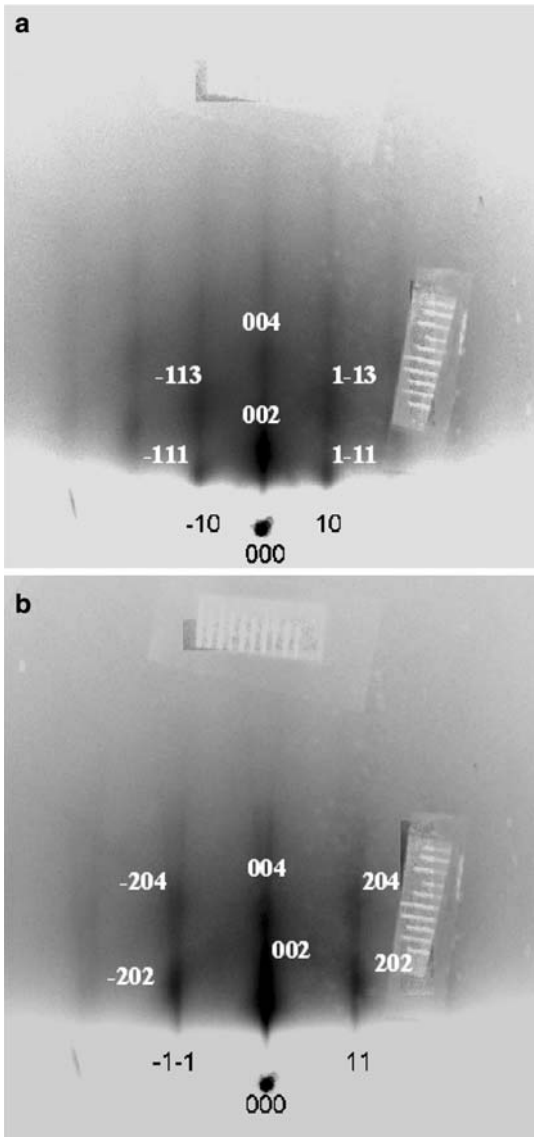

Fig. 2 RHEED patterns obtained from Pt (0.4 ML) on a thin film of Al_2O_3/NiAl(100). The patterns are obtained at (**a**) [0–10] and (**b**) [0–11] azimuths. The diffraction lines arise from the substrate and the diffraction spots from the Pt clusters; the assignment of these diffraction spots is based on the analysis in [20]

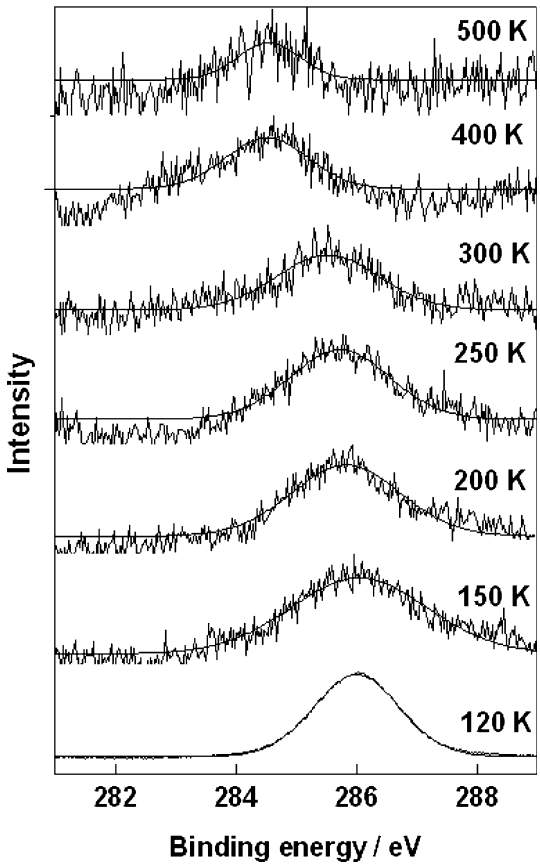

Fig. 3 Representative C 1s photoelectron spectra in a sequence acquired at 120 K for cyclohexene (1 L) adsorbed on Pt clusters (2 ML) supported on an Al_2O_3/NiAl(100) thin film and subsequently annealed to the temperatures indicated in the figure

Figure 4 displays also a comparison of the BE shift, total area and FWHM of the C 1s signal from cyclohexene (1 L) adsorbed on varied Pt coverages (0.2, 0.5 and 2 ML) to demonstrate the effect of Pt coverage on the dehydrogenation. According to Fig. 4(a), the behavior clearly varies with the Pt coverage. In the initial stage of dehydrogenation, the difference is minor, but the dissociation of benzene (the region about 284.5–285 eV) is completed at significantly lower temperatures with a small coverage of Pt. The FWHM variations corroborate this result. Figure 4(b) shows that the FWHM for Pt (0.2 ML) is decreased to the original value in the same temperature region, 220–300 K, as the benzene decomposition, also much lower than the temperature at the other Pt coverages. As the increase of FWHM indicates coexistence of various species (the resolution of the beamline remained the same throughout the experiment), the decrease of FWHM to the original value indicates that only one carbon species remains on the surface, which is elemental carbon according to its corresponding BE. The observed reduction of FWHM reflects the decomposition toward elemental carbon. Both BE and FWHM results thus indicate that Pt at a small coverage is more reactive for the hydrocarbon decomposition. As the cluster size and morphology vary insignificantly with the coverage [19], the variability of the reactivity might arise not solely from the variation of the cluster morphology: the reactivity might involve the oxide support. A comprehensive answer to this question requires further investigation. Figure 4(c) shows the quantities of the hydrocarbon species on the surface as a function of the annealing temperature. The trend for three coverages is nearly the same: following an abrupt decrease near 150 K, a continuously decreasing area of the C 1s signal was ob-

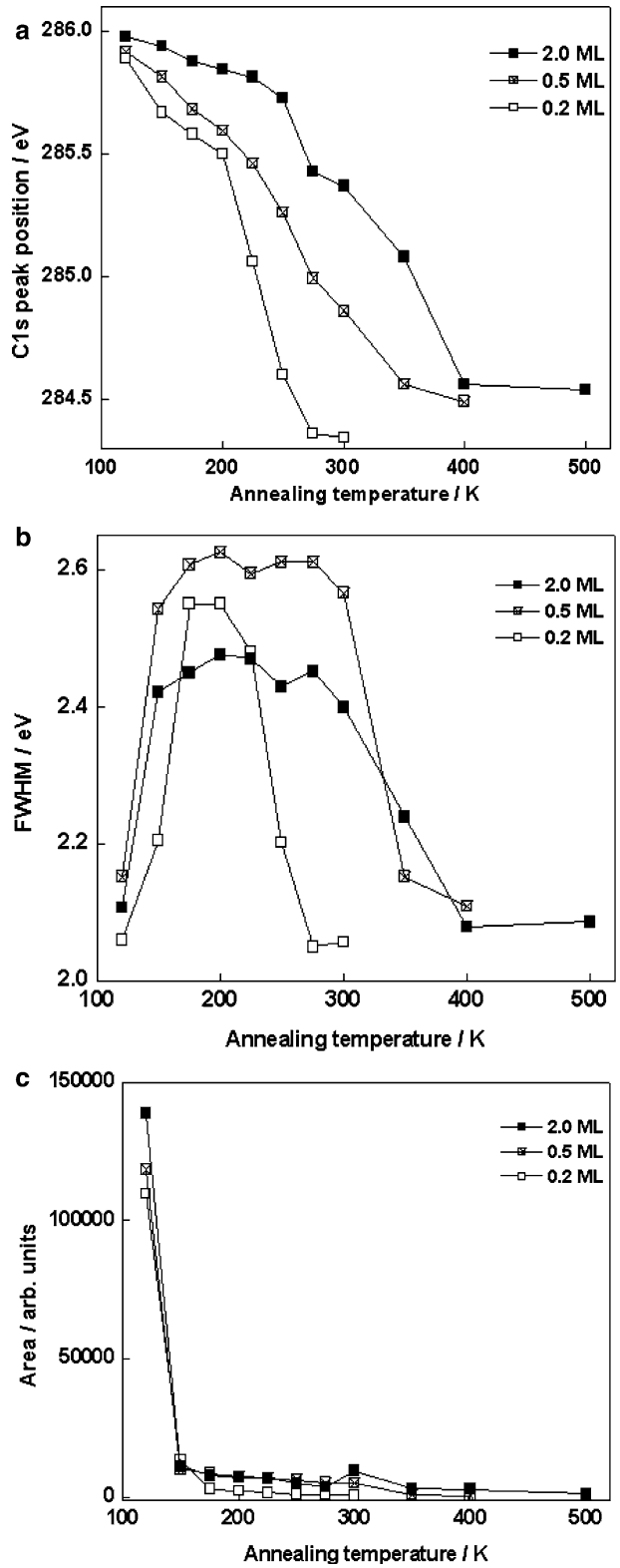

Fig. 4 Effect of coverage (0.2, 0.5 and 2 ML) of Pt nanoclusters formed at 300 K on the dehydrogenation of adsorbed cyclohexene (1 L). Variations of (**a**) C 1s signal position, (**b**) full width at half maximum (FWHM) of the C 1s signal and (**c**) area of the C 1s signal with annealing temperature

served, indicating that after the multilayer desorption both dehydrogenation and slow desorption occur concurrently.

To explore the effect of the temperature of cluster growth, we adsorbed cyclohexene (1 L) on Pt (2 ML) on an Al_2O_3/NiAl(100) thin film deposited at 300 or 450 or 600 K; the corresponding dehydrogenation features are indistinguishable. The BE, area and FWHM of their C 1s signals exhibit a similar dependence on the annealing temperature. As the growth temperature from 300 to 600 K does not much alter the size and morphology of the cluster, according to the STM observations [19], the major variation in these samples is the structural ordering in these clusters. The RHEED measurements indicate a greater structural ordering—sharper diffraction spots—for clusters formed at a higher temperature of growth. This result hence implies that the reactivity of the cluster is insensitive to the structural differences caused by the varied growth temperatures in such a range. As for the effect of dose (1–10 L) of cyclohexene on the dehydrogenation, multilayer cyclohexene desorbs after annealing to 150 K and a similar proportion of hydrocarbon remains. The remaining species showed the same dehydrogenation behavior as above for the subsequent annealing.

4 Conclusions

According to our analysis of observations from STM, RHEED and PES measurements on the dehydrogenation of cyclohexene adsorbed on Pt nanoclusters on a thin film of Al_2O_3/NiAl(100), the prepared Pt clusters are crystalline and have a mean diameter 2.2 nm and height 0.4 nm. Their size varies little with the coverage and the growth temperature. The dehydrogenation of the adsorbed cyclohexene exhibits a sequential process beginning near 150 K, a temperature significantly lower than that for Pt single crystals. Further annealing causes dissociation of benzene and leaves elemental carbon on the surface. Such dissociation occurs at temperatures also much lower than that on Pt single crystals. The dehydrogenation behavior, particularly the decomposition into elemental carbon, varies with the Pt coverage.

Acknowledgments National Science Council (under grants NSC 94–2112-M-008-032 and NSC 95-2811-M-008-018) and National Synchrotron Radiation Research Centre of Taiwan supported this work. We thank M. H. Ten, W. R. Lin, C. I. Chiang and Z. F. Lin for their technical assistance in the experiments.

References

1. Land DP, Pettiette-Hall CL, McIver RT, Hemminger JC (1989) J Am Chem Soc 111:5970
2. Pettiette-Hall CL, Land DP, McIver JRT, Hemminger JC (1991) J Am Chem Soc 113:2755

3. Parker DH, Pettiette-Hall CL, Li Y, McIver JRT, Hemminger JC (1992) J Phys Chem B 96:1888
4. Pansoy-Hjelvik ME, Schnabel P, Hemminger JC (2000) J Phys Chem B 104:554
5. Perry DA, Hemminger JC (2000) J Am Chem Soc 122:8079
6. Koel BE, Blank DA, Carter EA (1998) J Mol Catal A: Chem 131:39
7. Lamont CLA, Borbach M, Martin R, Gardner P, Jones TS, Conrad H, Bradshaw AM (1997) Surf Sci 374:215
8. Tsai MC, Friend CM, Muetterties EL (1982) J Am Chem Soc 104:2539
9. Bratlie KM, Flores LD, Somorjai GA (2005) Surf Sci 599:93
10. Montano M, Salmeron M, Somorjai GA (2006) Surf Sci 600:1809
11. Yang M, Rioux RM, Somorjai GA (2006) J Catal 237:255
12. Henry CR (1998) Surf Sci Rep 31:231
13. Bäumer M, Freund H-J (1999) Prog Surf Sci 61:127
14. Bell AT (2003) Science 299:1688
15. Santra AK, Goodman DW (2002) J Phys: Condens Matter 14:R31
16. Goodman DW (1995) Chem Rev 95:523
17. Heiz U, Bullock EL (2004) J Mater Chem 14:564
18. Sandell A, Libuda J, Brühwiler PA, Andersson S, Bäumer M, Maxwell AJ, Mårtensson N, Freund H-J (1997) Phys Rev B 55:7233
19. Sartale SD, Shiu HW, Ten MH, Huang JY, Luo MF (2006) Surf Sci 600:1942
20. Luo MF, Wen WH, Lin CS, Chiang CI, Sartale SD, Zei MS (2007) Surf Sci 601:2139
21. Luo MF, Chiang CI, Shiu HW, Sartale SD, Kuo CC (2006) Nanotechnol 70:360
22. Zei MS, Lin CS, Wei WH, Chiang CI, Luo MF (2006) Surf Sci 600:1942
23. Lai LJ, Tseng PC, Yang YW, Chung SC, Song YF, Cheng NF, Chen CC, Chen CT, Tsang KL (2001) Nuclear Instrum Methods Phys Res A 467–468:586
24. Moulder JF, Stickle WF, Sobol PE, Bomben KD (1995) Handbook of x-ray photoelectron spectroscopy. Physical Electronics, Inc, USA
25. Yeh J-J (1993) Atomic calculation of photoionization cross sections and asymmetry parameters. A T & T Bell Laboratories, USA
26. Rodriguez NM, Anderson PE, Wootsch A, Wild U, Schlögl R, Paál Z (2001) J Catal 197:365